Effect of varying electric potential on surface-plasmon resonance sensing

Vladimir Lioubimov, Alexandre Kolomenskii, Andreas Mershin, Dimitri V. Nanopoulos, and Hans A. Schuessler

The high sensitivity of surface-plasmon resonance (SPR) sensors allows measurements of small variations in surface potentials to be made. We studied the changes of the SPR angle when an oscillating electric potential was applied to a gold film on which surface plasmons were excited. The shifts of the SPR resonance angle were observed for various aqueous solutions as an adjacent medium. A model that takes into account the redistribution of charges at the double layer near the metal–liquid interface as well as the oxidation of the gold film was developed. It was found that a change in the electronic density at voltages below the oxidation potential and, in addition, the oxidation of the gold surface above this potential are the main mechanisms that account for the observed dependences. It was shown that relatively slow oxidation–reduction processes can explain the observed hysteresis effect. Application of these techniques to studies of dielectric properties and conformational changes of polar biomolecules, such as tubulin, are discussed.

OCIS codes: 170.3890, 270.0270, 240.6680, 230.0250.

1. Introduction

A recently developed sensing technique based on the surface-plasmon resonance (SPR) phenomenon[1–4] stimulated studies of different factors that affect the shift of the resonance angle at the SPR. In the most common Kretchmann geometry[2] the resonance interaction between the evanescent electromagnetic wave and the surface plasmons is achieved by matching their phase velocities along the surface. This is realized by using a prism in optical contact with a metal (gold) film and by selecting the value of the incidence angle of the excitation optical beam so that the efficient conversion of an incident photon into a surface plasmon is possible. The resonance angle depends on the complex dielectric constant of the metal film and on the dielectric properties of the media adjacent to this film. The application of an electric potential changes the dielectric properties in the vicinity of the metal–liquid interface, resulting in a variation in the SPR signal, an effect that has indeed been observed.[5–9] It has been shown[6] that the formation of a Helmholtz double layer influences the SPR response significantly. A change in the electric potential over a certain value initiates electrochemical reactions such as oxidation and reduction of the metal. In this work we measured the SPR shift in the Kretchmann configuration when the potential at the gold film was cycled with magnitudes below and above the oxidation potential. We developed a multilayer model that takes into account the changes in the dielectric properties near the interface. This model incorporates both changes due to the formation of the double layer and to the oxidation–reduction reactions.

The variations in the SPR angle with electric potential are important not only because they can affect the measurements with SPR sensors: The possibility to measure the electric field locally with an SPR technique that yields good spatial and temporal resolutions can be utilized in various bioscience applications. In our recent studies of protein structures, such as sarcomeres[10] (actinomyosin complexes that make up the basic units of muscle contraction) and tubulin dimers and polymers,[11] we found that SPR-based biosensors are capable of detecting changes in the bulk conformational state and of measuring minute changes in their dielectric constants. In the present paper we show that the application of an electric potential to the metal surface of the biosensor

The authors are with the Department of Physics, Texas A&M University, College Station, Texas 77843-4242. A. Kolomenskii's e-mail address is a-kolomenski@physics.tamu.edu.

Received 1 December 2003; revised manuscript received 15 March 2004; accepted 16 March 2004.

0003-6935/04/173426-07$15.00/0

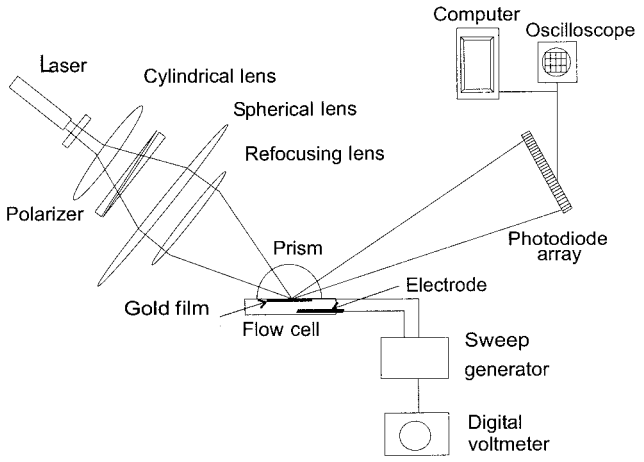

Fig. 1. Experimental setup.

chip can increase the sensitivity manyfold. In addition, knowledge of the effects of electric potentials on the SPR phenomenon paves the way for dynamic coupling of these effects to the dielectric properties of immobilized protein molecules and for monitoring them at the same time.

2. Experimental Setup

The experimental setup is shown in Fig. 1. A He–Ne laser provided the incident illumination at a wavelength of 633 nm. An arrangement of lenses and a polarizer produced a parallel-polarized light beam that converged in an angular interval adjusted to select a suitable dynamic range and resolution for the SPR angle. A prism was used to couple the laser beam to the surface plasmons that were excited on the gold film of a standard sensor chip (CM5, Biacore AB). A photodiode array (S3924-1024Q, Hamamatsu) captured the angular distribution of the reflected light. A data acquisition board (AT-MIO-16X, National Instruments) read the electrical output of the photodiode array and transferred it to a personal computer. In-house C software calculated in real time the SPR angle (corresponding to the minimum in the intensity distribution of the reflected light) and stored the data. The readout rate was faster than 10 s^{-1}. The measured beam spot size at the sensor chip was 0.15 mm^2. One pixel on the photodiode array corresponded to $\sim 6 \times 10^{-3}$ deg. A flow cell with channel dimensions of 5 mm $\times$ 1 mm $\times$ 1 mm interfaced with the surface of the gold film.

The experiments were performed with a periodically cycling linear sweep of the potential applied to the metal surface. Compared with changing the potential in discrete DC voltage steps, this approach allowed us to obtain a much better reproducibility of the data, because the processes at the interface are time dependent. One electrode was a steel rod positioned inside the cell, whereas the other electrode was the gold surface of the chip itself. The electrodes were connected to a stabilized sweep generator.

The potential is referred to as positive when positive voltage is applied to the gold surface. The liquids we used were distilled water, propeonic acid, and aqueous solutions of potassium hydroxide (KOH) and NaCl. The applied voltage was varied within the range from -1.5 to $+1.5$ V, which included regions below and above the oxidation potential. The repetition rate of the sweeping potential was 0.002 Hz in all measurements, except for the case in which we studied the frequency dependence. In some measurements the oxidation process was avoided by appropriately reducing the magnitude of the potential variations.

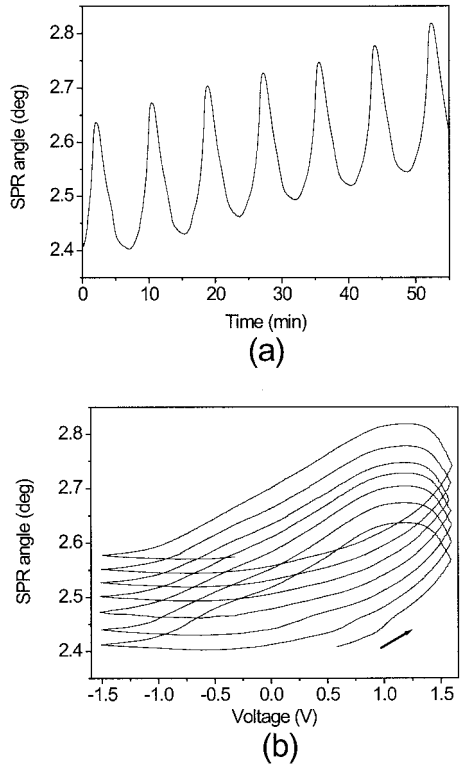

Fig. 2. Angle variations of the SPR for pure water with voltage sweeping from -1.5 to 1.5 V: (a) time dependence and (b) voltage dependence. The arrow in (b) indicates the direction of the process in time.

3. Experimental Results

The SPR angle shift, i.e., the change in the angular position of the resonance, was studied as a function of time and applied voltage. The results for different solutions are presented in Figs. 2–6. The amplitude of the SPR shift in the positive range of the sweep potential (up to $\sim$1.5 V) varies for different solutions: 0.158 deg for pure water (Fig. 2), 0.204 deg for 5-mM propeonic acid (Fig. 4), 0.318 deg for the 5-mM KOH solution (Fig. 3), and 0.420 deg for the 5-mM NaCl solution (Fig. 5). Note that the voltage dependences of the SPR shift are qualitatively similar for all the solutions measured: The portion of the curve corresponding to the negative voltage changes only slightly, whereas for positive voltages the ascending branch of the dependence curve goes lower than the descending branch (hysteresis).

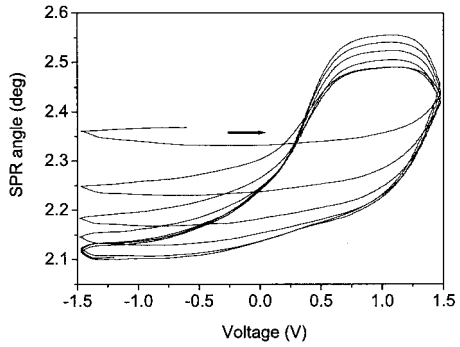

Fig. 3. Angle variations of the SPR for the 5-mM KOH aqueous solution with voltage sweeping from −1.5 to 1.5 V. The arrow indicates the direction of the process in time.

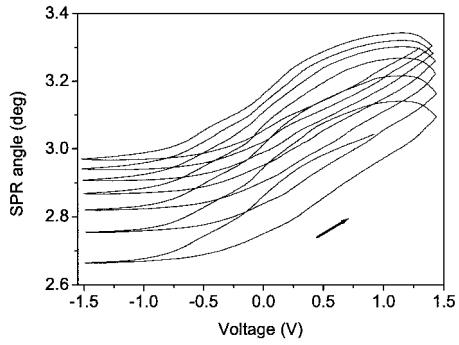

Fig. 5. Angle variations of the SPR for the 5-mM NaCl aqueous solution with voltage sweeping from −1.5 to 1.5 V. The arrow indicates the direction of the process in time.

The pure-water SPR shift that is induced by the potential below the oxidation threshold is shown in Fig. 6. In this case the magnitude of the 0.031-deg SPR shift is much smaller than the 0.158-deg shift observed when the voltage exceeded the oxidation potential (Fig. 2). The same effect takes place for the 0.5-mM aqueous solution of NaCl. When we varied the applied voltage from −0.8 to +0.8 V, the shift of the resonance angle was only 0.024 deg (data not shown) compared with 0.42 deg when the voltage range was from −1.5 to +1.5 V (Fig. 5).

By comparing the results for pure water (Fig. 2) with those for the 5-mM NaCl solution (Fig. 5), we conclude that the difference in the magnitude of the SPR shift oscillations is 0.18 deg. The same change in concentration without the application of an electric potential causes a SPR shift of only ~0.006 deg.[12] Thus, by applying an electric potential, one can achieve approximately a 30-fold improvement in the measurements' sensitivity to changes in solution concentration. This enhancement of the sensitivity is frequency dependent and is larger at lower frequencies. To better understand the kinetics of the processes occurring at the metal–liquid interface, we performed the experiments with different sweep rates of the applied potential (Fig. 7). The SPR shift decreased with increasing cycle frequency: for a frequency of 0.02 Hz it was 0.078 deg, compared with the SPR shift of only 0.003 deg for a higher-sweeping frequency of 0.2 Hz and a shift of 0.138 deg for a lower-sweeping frequency of 0.002 Hz.

4. Theoretical Model

The physical and chemical phenomena that occur when an electric field is applied at the metal–dielectric interface have been extensively discussed in the literature (see Ref. 13 and the references therein). Different mechanisms take place at this interface and can be responsible for the angle shift of the SPR, namely, formation of the Helmholtz double layer, changes in the electronic density, and oxidation of the metal film. These phenomena also depend on the solution that is in contact with the metal.

A. Double Layer

From the Boltzmann distribution of electric charges and Gauss's law of electrostatics, and according to Gouy–Chapman theory, it was derived that the surface charge density at the metal–electrolyte interface is equal to[13]

$$\sigma = (8kT\epsilon\epsilon_0 n)^{1/2}\sinh\frac{ze\psi_0}{2kT}, \qquad (1)$$

where k is the Boltzmann constant, T is the absolute temperature, ϵ is the dielectric constant of the electrolyte solution, ϵ_0 is the permittivity of vacuum, n is

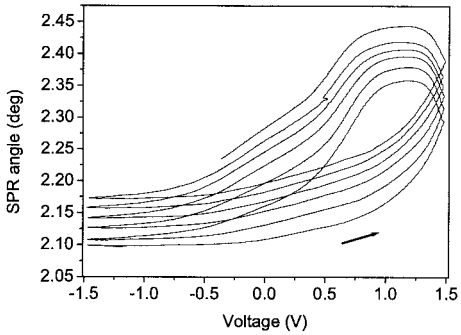

Fig. 4. Angle variations of the SPR for the 5-mM propeonic acid aqueous solution with voltage sweeping from −1.5 to 1.5 V. The arrow indicates the direction of the process in time.

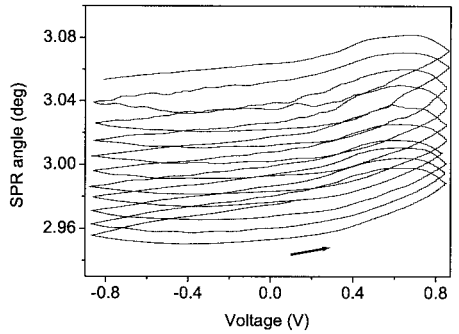

Fig. 6. Angle variations of the SPR for pure water with voltage sweeping from −0.8 to 0.8 V. The arrow indicates the direction of the process in time.

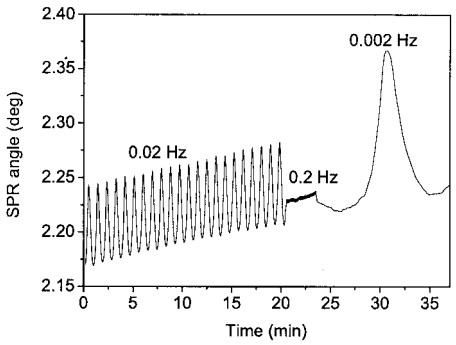

Fig. 7. Angle variations of the SPR for pure water with voltage sweeping from −1.5 to 1.5 V at different sweep-potential rates.

the bulk concentration of charges, z is the valence of the electrolyte, e is the elementary electric charge, and ψ_0 is the value that the electric potential ψ acquires at the metal–electrolyte interface $x = 0$.

However, the implementation of Eq. (1) gives values of σ that are too large for a potential of the order of 1 V. This difficulty was overcome by Stern (see Ref. 13), who assumed that, immediately adjacent to the interface, there is a thin layer with a constant electric field. In this layer the potential linearly changes from the value ψ_0 at the interface to the value ψ_2 on the other side of the layer. Adjacent to this layer is the diffuse region called the outer-Helmholtz layer.[13] Thus potential at the interface of these two regions is

$$\psi_2 = \left(\frac{d\psi}{dx}\right)_{x=x_2} x_2 + \psi_0, \tag{2}$$

where

$$\left(\frac{d\psi}{dx}\right)_{x=x_2} = -\left(\frac{8kTn}{\epsilon\epsilon_0}\right)^{1/2} \sinh\frac{ze\psi_2}{2kT}. \tag{3}$$

By solving Eqs. (2) and (3) numerically, the surface charge density $\Delta\sigma$ was determined for each value of the surface potential ψ_0.

McIntyre[14] proposed a model describing the changes in the dielectric constant of a metal in terms of variations in the electronic density:

$$\Delta\epsilon_m = (\epsilon_e - 1)\frac{\Delta n}{nd}, \tag{4}$$

where ϵ_e is the free-electron contribution to the dielectric constant of the metal, n is the free-electron density of the bulk metal, d is the penetration depth of the electric field into the metal, and Δn is the excess electronic density in the surface layer:

$$\Delta n = -\frac{\Delta\sigma}{ed}. \tag{5}$$

Consequently, the dielectric constant of the metal can be presented as

$$\epsilon_m = \epsilon_{m0} + \Delta\epsilon_m, \tag{6}$$

where ϵ_{m0} is the unperturbed dielectric constant of the metal and $\Delta\epsilon_m$ describes the changes induced by the surface-potential variations.

B. Multilayer Model of the Surface-Plasmon Resonance

The change in the dielectric constant of the metal can be related to the SPR shift. We model our system as consisting of n layers, each having its own thickness d_i and complex dielectric constant ϵ_i. The reflection coefficient R for this system can be calculated[15] as

$$R = \left|\frac{Z_{in,2} - Z_1}{Z_{in,2} + Z_1}\right|^2, \tag{7}$$

by use of recursive relations for the input impedance $Z_{in,m}$ at layer m and the layer impedance Z_m,

$$Z_{in,m} = Z_m\left(\frac{Z_{in,m+1} - iZ_m \tan k_{Z,m}d_m}{Z_m - iZ_{in,m+1}\tan k_{Z,m}d_m}\right) \tag{8}$$

for m from 2 to n. For the last layer n, $Z_{in,n} = Z_n$, and for an arbitrary in-between layer m the following relations are valid: $k_{Z,m} = (\epsilon_m k_0^2 - k^2)^{1/2}$ and $Z_m = k_{Z,m}/\epsilon_m k_0$. The wave-vector component parallel to the prism–metal interface depends on the incidence angle θ: $k = k_0(\epsilon_1)^{1/2}\sin\theta$, where $k_0 = 2\pi/\lambda$ and λ is the wavelength of the laser light in vacuum.

We assume that the main change in the dielectric properties at optical frequencies is related to the contribution of the free electrons in the metal. Two processes affecting the dielectric properties of the metal film were considered: the formation of the double layer and the oxidation of gold. We consider a four-layer model consisting of the following: first layer, prism with dielectric permittivity $\epsilon_1 = 2.3$; second layer, gold film of thickness $d_2 = 47$ nm with complex permittivity $\epsilon_2 = -13.2 + i1.25$; third layer, thin surface region of gold with the thickness equal to the penetration depth of the quasi-static electromagnetic field into the metal of thickness $d_3 = 0.1$ nm[6], where the electronic charge density is modified and induced by the double layer change $\Delta\epsilon_m$; fourth layer, liquid only with $\epsilon_5 = 1.777$ (this layer is assumed to be semi-infinite with respect to the surface-plasmon penetration depth).

The magnitude of the SPR shifts that follow from the multilayer model used together with Eqs. (7) and (8) is close to the experimental results obtained at voltages below the oxidation potential. With $x_2 = 5$ Å (close to the 3.7-Å value accepted for the Stern layer reported previously[13]), the model calculations for the SPR shift yield $\Delta\theta = 0.05$ deg at a voltage of 0.8 V, whereas the experimental values are $\Delta\theta = 0.031$ deg (Fig. 6) and $\Delta\theta = 0.05$ deg (Fig. 2). For the potential sweeps above the oxidation potential, the double layer alone cannot account for the observed SPR shift. At a voltage of 1.5 V the experimental value of the SPR shift is 0.158 deg (Fig. 2). For the same voltage, the contribution of the double layer alone yields a value of 0.106 deg. To account for the contribution of the oxidation process, we introduced an additional (oxide) 3-Å-thick layer between layers 3

and 4 (the thickness of the gold layer was correspondingly reduced). Layers of oxidized gold several angstroms in thickness were reported previously.[16] The dielectric constant of this oxide layer is accepted to be $\epsilon_3 = 1.44 - i0.3$, which is within the range of the values reported in the literature.[16] The oxide layer provides an additional 0.052-deg shift so that the total calculated value $\Delta\theta = 0.158$ deg is in agreement with the experimental one.

C. Dynamics of the Oxidation Process

The oxidation process is greatly dependent on the chemical content of the solution as well as on the range and the frequency of the potential sweep. In acidic solutions the anodic polarization of the gold electrode takes place,[16] leading to the formation of Au_2O_3 oxide on the electrode:

$$Au_2O_3 + 6H^+ + 6e \rightleftharpoons 2Au + 3H_2O. \quad (9)$$

The Au_2O_3 oxide is a poorly adherent species, has a flaky nature, and is reddish-brown to black in color. The reaction of the oxide formation starts at 1.35 V, whereas the reduction reaction starts at 1.1 V.[16]

We model the dynamics of the oxide layer by using the diffusion equation

$$\frac{\partial C}{\partial t} = D\,\frac{\partial^2 C}{\partial x^2}, \quad (10)$$

where C is the oxide concentration and D is the diffusion coefficient characterizing the oxidation process. In addition, the boundary condition $C(0, t) = f(t), t \geq 0$ at the surface and the initial condition $C(x, 0) = 0, 0 \leq x < \infty$ should be satisfied. The substitution of a metal film by a half-space is justified in our case owing to sweep periods that are shorter than the diffusion time of the oxidation process through the metal film. We assume that the boundary concentration for a linearly increasing potential is changing as a linear function $f(t) = bt$. Then, applying a Laplace transformation to the diffusion equation, we obtain for the oxide concentration

$$C(x, t) = b\int_0^t erfc\,\frac{x}{\sqrt{4Dt}}\,\mathrm{d}t. \quad (11)$$

The total amount of the oxide (and thus the efficient thickness of the oxide layer per unit area) is proportional to the integral of the concentration C over the entire depth. Given that

$$\int_0^\infty C\mathrm{d}x = b\int_0^\infty \mathrm{d}x\int_0^t\left(1 - \frac{2}{\sqrt{\pi}}\int_0^{\frac{x}{\sqrt{4Dt}}} e^{-z^2}\mathrm{d}z\right)\mathrm{d}t$$

$$= \int_0^t \sqrt{4Dt}\mathrm{d}t \times b = 0.376b \times (4Dt)^{3/2}, \quad (12)$$

the SPR shift that is related to the integral amount of the oxide formed is also proportional to $t^{3/2}$. A similar solution can be used during the second phase of the voltage sweep, when the potential linearly decreases, with an additional assumption that the surface concentration decreases proportionally too. During this second phase, in the range of the positive potentials, the SPR shift changes in time as $\sim[t^{3/2} - \theta(t - t_0)(t - t_0)^{3/2}]$, where time t_0 corresponds to the voltage maximum and $\theta(t)$ is the unit step function. This dependence, shown in Fig. 8, demonstrates a good qualitative agreement with the experimentally observed temporal behavior of the SPR shift near the voltage maximum (compare Figs. 8 and 5).

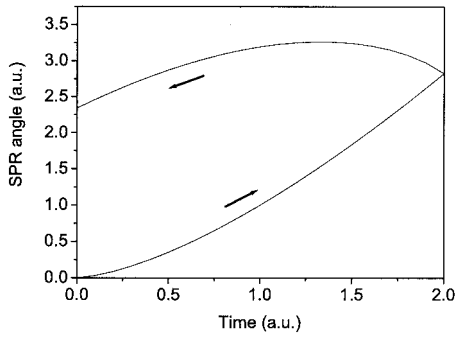

Fig. 8. Result of the calculation of the SPR shift with the diffusion model of the oxidation–reduction process. The arrows indicate the direction of the process in time. This dependence clearly shows hysteresis, which was also observed experimentally.

5. Discussion

We measured the characteristic shape of the dependence curve for the SPR shift on voltage, with a flattening of the curve observed for negative voltages for all investigated liquids. This dependence was discussed previously by Kolb.[17] He pointed out that the negative potential does not lead to a decrease in the electronic concentration, but rather induces an expulsion of some portion of an electronic cloud from the metal, thereby making the electronic density almost constant. In contrast, a positive electric potential leads to an attraction of additional electrons to the surface region. This is accompanied by an increase in the electronic density and results in an increase in the SPR angle. Indeed, such an increase was observed in our experiments. However, our calculations have shown that the increase in the electronic density by itself is insufficient to account for the total SPR shift at higher voltage values. Furthermore, the potential-induced changes in the electronic density present a reversible mechanism that does not explain the observed hysteresis. A better agreement was obtained when we took into account the oxidation process. We also considered the dynamics of the oxidation–reduction processes, which we introduced in our description by implementing the diffusion model. This model not only explained the observed hysteresis but also yielded a SPR response curve for positive voltages that was similar in shape to the experimental one (compare the experimental curves in Figs. 2 and 5 with the theoretically calculated dependence in Fig. 8).

During each voltametric cycle, after the oxidation

of a gold layer, the reduction process proceeds with some retardation, which results in an irreversibility of the SPR shift and the resulting hysteresis effect. Once the cycle is complete, the thickness of the oxide layer can be different from what it was at the beginning of the cycle, and thus the SPR curve can be slightly shifted, as indeed was observed experimentally. The average SPR angle shift observed for consecutive cycles, even at voltages below the oxidation potential (Fig. 6), indicates that there is no abrupt threshold for the onset of the oxidation process. This fact can be related to the polycrystalline structure of the gold film.[18] With an increase in the number of cycles, the shifts after each cycle became smaller and smaller, indicating that the thickness of the oxide layer was approaching some quasi-equilibrium value. In addition, our theoretical model predicts a frequency dependence $\sim f^{-\gamma}$, where $\gamma = 1.5$, for the magnitude of the positive SPR shift. In our experiments we observed a decrease in the SPR shift by a factor of 30 with a frequency increase by a factor of 10. This gives a value of $\gamma = 1.48$, which is very close to the predicted γ.

Variations in the electric potential can also occur in biomolecular systems such as, for instance, the microtubular cytoskeleton that can be assembled on a SPR chip.[11] In microtubule (MT) dynamics models, it is often calculated that electric fields of the order of 10^5 V/m are present in and around MTs[19] owing to the ferroelectric behavior of the constituent tubulin dipoles[20] and to the membrane potentials. Such fields and their associated potentials can be studied by monitoring the SPR angle shifts that they induce. Conversely, a MT can experience longitudinal forces if an external electric field is applied along an MT network. Depending on direction, this tends to stretch, compress, or realign the MT, giving the experimenter a way to induce polymerization of MTs in particular patterns, including nodes and networks. *In vitro* experiments showing that MTs react (by at least orienting) to electric fields have been performed,[21,22] but synchronous monitoring of their polymerization dynamics has never been attempted. A refined implementation of the techniques described here could allow synchronous application of a voltage and monitoring of the SPR angle, which would depend on the length of the MT, and thus could help to characterize the polymerization state. Electrical, especially dipole–dipole, interactions are important to (de)polymerization dynamics. The calculated value of the permanent electric dipole moment of the tubulin molecule (of the order of 1700 Debye)[19] yields an interaction energy between two neighboring tubulin dimers (center-to-center distance of the order of 8 nm) to be of the order of 15 eV, whereas the thermal noise energy is 0.025 eV and the guanosine 5′-triphosphate hydrolysis energy is 0.42 eV. Because the dipole moment of a protein is related to its dielectric constant and the SPR angle is very sensitive to the local dielectric constant at the metal–liquid interface, SPR measurements of dipole interactions and polymerization dynamics are feasible. Furthermore, combined studies of membrane potential measurements[23] and conformational changes can be designed so that the SPR signal reports both the potential across a membrane and the conformation of transmembrane proteins.

6. Conclusion

The behavior of the SPR response to the application of cycling electric potential was studied. For a positive potential at the metal (gold) surface, a significant shift in the SPR angle occurred owing to the change in the electronic concentration and the related change in the dielectric properties of the metal. However, the observed SPR shifts can be only partially accounted for by the change in the electronic density in the metal. The observed hysteresis behavior of the SPR shift versus the voltage dependence also cannot be explained by the changes in the electronic density of the metal alone. We have shown that relatively slow chemical oxidation–reduction processes can explain the hysteresis phenomenon. The model based on the diffusion equation gave a good qualitative agreement with the observed hysteresis curve. By implementing biosensors with voltametric control of the surface layer and by taking into account the effects of electric potential on the SPR, the manipulation and monitoring of the dynamics and conformational changes of protein complexes, such as sarcomeres and microtubules, can eventually be realized.

This work was partially supported by a grant from the Telecommunications and Informatics Task Force from Texas A&M University and by National Science Foundation grant 0218595. A. Mershin was partially supported by a scholarship from the A. S. Onassis Public Benefit Foundation.

References

1. A. Otto, "Excitation of nonradiative surface plasma waves in silver by the method of frustrated total reflection," Z. Phys. **216,** 398–410 (1968).
2. E. Kretschmann, "Die Bestimmung optischer Konstanten von Metallen durch Anregung von Oberflachenplasmaschwingungen," Z. Phys. **241,** 313–324 (1971).
3. J. R. Sambles, G. W. Bradbary, and Fuzi Yang, "Optical excitation of surface plasmons: an introduction," Contemp. Phys. **32,** 173–183 (1991).
4. U. Jonsson, L. Fagerstam, B. Ivarsson, B. Johnsson, R. Karlsson, D. Persson, H. Ross, I. Ronnberg, S. Sjolander, E. Stenberg, R. Stahlberg, C. Urbaniczky, H. Ostlin, and M. Malmqvist, "Real-time biospecific interaction analysis using surface plasmon resonance and sensor chip technology," BioTechniques **11,** 620–627 (1991).
5. F. Abeles and T. Lopez-Rios, "Investigation of the metal-electrolyte interface using surface plasma waves with ellipsometric detection," Solid State Commun. **16,** 843–847 (1975).
6. R. Kotz, D. M. Kolb, and J. K. Saas, "Electron density effects in surface plasmon excitation on silver and gold electrodes," Surf. Sci. **69,** 359–364 (1977).
7. J. G. Gordon and S. Ernst, "Surface plasmons as a probe of the electrochemical interface," Surf. Sci. **101,** 499–509 (1980).
8. A. Tadjeddine, D. M. Kolb, and R. Kotz, "The study of single crystal electrode surfaces by surface plasmon excitation," Surf. Sci. **101,** 277–285 (1980).

9. A. Tadjeddine, "Influence of the electrical polarization on the surface plasmon dispersion at metal electrolyte interfaces," Electrochim. Acta **34,** 29–33 (1989).
10. C. W. Tong, A. Kolomenskii, V. Lioubimov, H. A. Schuessler, A. Trache, H. J. Granger, and M. Muthuchamy, "Measurements of the cross-bridge attachment detachment process within intact sarcomeres by surface plasmon resonance," Biochemistry **40,** 13915–13924 (2001).
11. H. A. Schuessler, A. Mershin, A. A. Kolomenskii, and D. V. Nanopoulos, "Surface plasmon resonance study of the actin–myosin sarcomeric complex and tubulin dimers," J. Mod. Opt. **50,** 2381–2391 (2003).
12. A. A. Kolomenskii, P. D. Gershon, and H. A. Schuessler, "Sensitivity and detection limit of concentration and adsorption measurements by laser induced surface plasmon resonance," Appl. Opt. **36,** 6539–6547 (1997).
13. H. Ohshima and K. Furusawa, "Electrical phenomena at interfaces," Surf. Sci. Ser. **76,** 1–17 (1998).
14. J. McIntyre, "Electrochemical modulation spectroscopy," Surf. Sci. **37,** 658–682 (1973).
15. L. M. Brekhovskikh, *Waves in Layered Media*, 2nd ed. (Academic, New York, 1980).
16. G. Belanger and A. K. Vijh, "Anodic oxides on noble metals," Anodic Beh. Metals Semiconductors Ser. **5,** 53–74 (1977).
17. D. M. Kolb and R. Kotz, "Electroreflectence spectra of Ag(III) electrode," Surf. Sci. **64,** 96–108 (1977).
18. A. S. Dakkouri and D. M. Kolb, "Reconstruction of gold surfaces," in *Interfacial Electrochemistry* (Marcel Dekker, New York, 1999), pp. 151–174.
19. N. E. Mavromatos, A. Mershin, and D. V. Nanopoulos, "QED-cavity model of microtubules implies dissipationless energy transfer and biological quantum teleportation," J. Mod. Phys. B **16,** 3623–3642 (2002).
20. M. V. Sataric, J. A. Tuszynski, and R. B. Zakula, "Kink-like excitations as an energy transfer mechanism in microtubules," Phys. Rev. E **48,** 589–587 (1993).
21. J. Pokorny, F. Jelinek, and V. Trkal, "Electric field around microtubules," Bioelectrochem. Bioenerg. **45,** 239–245 (1998).
22. F. Jelinek, J. Pokorny, J. Saroch, V. Trkal, J. Hasek, and B. Palan, "Microelectronic sensors for measurement of electromagnetic fields of living cells and experimental results," Bioelectrochem. Bioenerg. **48,** 261–266 (1999).
23. L. Gu, O. Braha, S. Conlan, S. Cheley, and H. Bayley, "Stochastic sensing of organic analytes by a pore-forming protein containing a molecular adapter," Nature **389,** 686–690 (1999).